Kinetics of *p*-Xylene Liquid-Phase Catalytic Oxidation

Giacomo Cao and Alberto Servida
Dipartimento di Ingegneria Chimica e Materiali, Universitá di Cagliari, Piazza d'Armi, 09123 Cagliari, Italy

Massimo Pisu
Centro di Ricerche, Sviluppo e Studi Superiori in Sardegna, Via Nazario Sauro 10, 09123 Cagliari, Italy

Massimo Morbidelli
Dipartimento di Chimica Fisica Applicata, Politecnico di Milano, Piazza Leonardo da Vinci 32, 20133 Milano, Italy

A semibatch gas-liquid reactor model based on a lumped kinetic scheme for the liquid-phase oxidation of p-xylene to p-toluic acid catalyzed by cobalt naphtenate is developed. The model accounts for the complex nature of the involved reaction network, as well as for the interphase and intraphase mass transport processes of both reactants and products. The model reliability is tested by comparison with suitable experimental data obtained in a semibatch oxidation reactor, where the role of the composition of both the gaseous and the liquid feed has been investigated. It is shown that the model describes the reactor behavior in any of the regimes which may prevail depending upon the operating conditions and the depletion of liquid reactants in time.

Introduction

Several industrial petrochemical processes are based on the liquid-phase catalytic oxidation of organic compounds by molecular oxygen, which can be either homolitic or heterolitic, depending upon the mechanism of oxygen activation (cf. Emanuel and Gal, 1986). Homolitic oxidation processes (for example, cyclohexanone and cyclohexanol from cyclohexane, terephtalic acid from *p*-xylene) have received great attention in the literature with particular emphasis on the catalytic system (that is, catalyst and promoter concentration, nature of the solvent, reaction temperature, and so on) and its influence on the oxidation rate (cf. Sheldon and Kochi, 1981; Raghavendrachar and Ramachandran, 1992). In large-scale reactors, the oxidation rate is in general determined by the simultaneous occurrence of chemical reactions and interphase and intraphase transport processes. The interactions between mass-transfer resistances and chemical reactions has been extensively examined in the context of gas-liquid absorbers (cf. Astarita et al., 1983), where the focus is on the overall uptake of the gaseous component, rather than on the product composition in the liquid phase. Accordingly, the available approximated solutions of the diffusion-reaction problem refer to very simple kinetic schemes, such as two parallel or consecutive reactions, and provide only the overall absorption rate of the gaseous reactant (cf. Doraiswamy and Sharma, 1984). Unfortunately, these results cannot be used to describe the product distribution in liquid-phase catalytic oxidations, whose kinetic mechanisms in general are rather complex (cf. Emanuel and Gal, 1986).

On the other hand, the formulation of detailed kinetic models of the oxidation process which describe all the involved elementary reactions and all the intermediate products is not desirable in practice. This is mainly because the estimation of the kinetic parameters of the elementary reactions by fitting of the experimental data cannot be performed when the concentrations of the participating components (that is, the radical species in the liquid phase) cannot be measured. In addition, the development of simulation models for gas-liquid oxidation reactors requires the solution of the diffusion-reaction equations in the film at the gas-liquid interface as well as the continuity equations for both gaseous and liquid bulk phases (cf. Carrá and Morbidelli, 1987). Then in order to keep low the

Correspondence concerning this article should be addressed to Massimo Morbidelli.
Current address of A. Servida: Istituto di Chimica Industriale, Universitá di Genova, C.so Europa 30, 16132 Genova, Italy.

computational effort, we need to adopt simplified (or lumped) kinetic schemes. This issue has been widely addressed in the literature (for example, Cavalieri d'Oro et al., 1980 for *p*-xylene oxidation; Chen et al., 1985 for *o*-xylene oxidation; Morbidelli et al., 1986 for ethylbenzene autoxidation; Krzysztoforski et al., 1986 for cyclohexane oxidation) with the goal of formulating lumped kinetic schemes which are simple but yet provide a description of the product distribution sufficient to evaluate the performance of industrial processes.

It is well established that the oxidation reaction of alkylaromatics is zeroth-order with respect to oxygen, as long as the oxygen partial pressure does not drop below a minimum value. In most cases this limit is given by 50–100 Torr (cf. Uri, 1961; Mill and Hendry, 1980). This is a direct consequence of the specific chain radical mechanism followed by these oxidation reactions, and in particular of the higher reactivity of the methyl radical with respect to that of the peroxide radical. Indeed, in the operating conditions of practical interest, the reaction rate is usually sufficiently large to lead to complete oxygen consumption somewhere in the liquid film. Thus, in this region the reaction order with respect to oxygen becomes larger than zero. However, as discussed by Morbidelli et al. (1984) and (1986), the contribution of this portion of the liquid film to the overall conversion in the reactor is so small that the zeroth-order kinetic model can be confidently used to simulate the performance of gas-liquid oxidation reactors.

The oxidation process can be either chemically rate limited or mass-transfer limited. At sufficiently high partial pressure of oxygen, the chemical rate controls the overall process and the apparent activation energy is usually in the range of 15–25 kcal/mol. On the other hand, at low oxygen partial pressure mass transfer may be the controlling process and the overall activation energy drops to about 3–5 kcal/mol (cf. Doraiswamy and Sharma, 1984). In this case the global reaction rate of the oxidation process depends upon oxygen partial pressure. In particular, in the case of liquid-phase oxidation of methylethylketone with air in a bubble column. Hobbs et al. (1972) found that at certain temperature values two zones where the overall oxidation rate is chemically and mass-transfer controlled can coexist in the column. The oxidation process in these two zones was simulated using two distinct kinetic models assuming zeroth- and first-order with respect to oxygen partial pressure, respectively. In the case of *p*-xylene oxidation catalyzed by cobalt naphtenate, Jacobi and Baerns (1983) have studied the effect of oxygen mass-transfer limitations on both the overall oxidation rate and the product distribution. A single kinetic model able to represent all the data could not be found. In fact the rate of *p*-xylene consumption was found to be proportional to the second power of *p*-xylene concentration in the chemically controlled regime, while a more complex expression, including the oxygen partial pressure as well as the *p*-xylene concentration, was proposed in order to represent the kinetic data in the presence of oxygen transfer limitations. These interpretations appear to be somehow contradictory because it is difficult to accept on physical grounds that a single kinetic model for the liquid-phase oxidation reactions is not sufficient, when coupled with a proper description of the mass-transfer processes, to describe the reactor behavior in all possible operating regimes.

In this work we consider the liquid-phase oxidation of *p*-xylene to *p*-toluic acid, catalyzed by cobalt naphtenate. This reaction has important practical implications since it constitutes the first step of the industrial process for the production of terephtalic acid. A lumped kinetic scheme is developed which accounts for the most important intermediates and final products of the process. All the involved reactions are assumed to be zeroth-order with respect to the gaseous reactant and first-order with respect to the liquid reactant. The developed reactor model, which accounts for the interphase and intraphase mass transport processes of both reactants and products, allows for the description of the reactor behavior in any of the regimes (that is, chemical or mass-transfer controlled) which may prevail depending upon the operating conditions. The reliability of the developed kinetic model is illustrated by comparison with experimental data obtained in a semibatch oxidation reactor where both the gas and the liquid phase are well mixed.

Experimental Procedure and Setup

The experimental setup used in this work is shown in Figure 1. The jacketed glass reactor was maintained at the desired temperature through forced circulation of water or diathermic oil; both the liquid and the gaseous phase were continuously stirred. The system was also equipped with a condenser in order to ensure complete condensation and recycle of the evaporated compounds. The reactor temperature was continuously recorded during the experimental runs through a thermocouple. In a typical experimental run, the reactor was charged with 200 cm^3 of *p*-xylene and 200 cm^3 of methyl benzoate. After the temperature reached the desired value, the catalyst (0.3 cm^3 of cobalt naphtenate) and a small amount of *p*-tolualdehyde (6 cm^3) were added. The gas (pure oxygen or air) was then continuously fed through the liquid. Methyl benzoate was used as a solvent in order to prevent the precipitation of *p*-toluic acid, which otherwise occurred in a crystalline form at conversions greater than about 15%. The reaction products were analyzed by high-pressure liquid chromatography (HPLC), equipped with a UV array detector and a reverse phase column (SPHERISORB ODS2) packed with unpolar C_{18}-hydrocarbons on silica gel (particle size 5 μm, column length 25 cm) and using cumene as internal standard. The column was operated at room temperature. A gradient elution was adopted to optimize the separation of the products. In particular, an eluent mixture of 17% methanol, 25% acetonitril, 0.1% phosphoric acid, and 58% water was fed into the column for 15 min followed by a mixture of 17% methanol, 44%

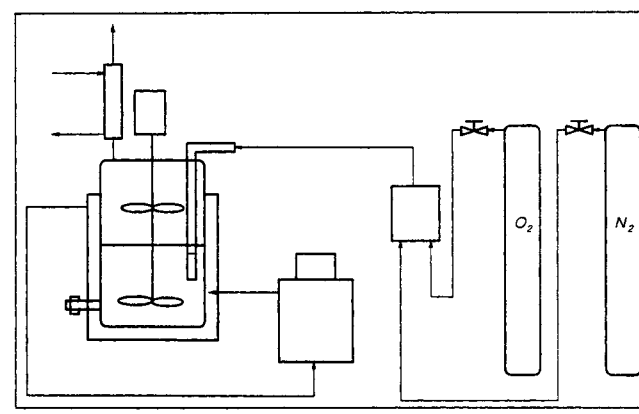

Figure 1. Experimental setup.

Table 1. Operating Conditions for the Experimental Runs

Run	T(°C)	C^{o}_{XY} (mol/kg$_{sol}$)	C^{o}_{TALD} (mol/kg$_{sol}$)	P_{gO_2} (atm)	N(rpm)
1	80	4	0.11	1	800
2	80	4	0.11	0.21	800
3	90	4	0.11	1	800
4	90	4	0.11	0.21	800
5	100	4	0.11	1	800
6	100	4	0.11	0.21	800
7	100	6	0.11	1	800
8	105	4	0.11	1	800
9	105	4	0.11	0.21	800
10	110	4	0.11	1	600
11	110	4	0.11	1	800
12	110	4	0.11	1	1,000
13	110	4	0.11	0.21	800
14	120	4	0.11	1	800
15	120	4	0.11	0.21	800

acetonitril, 0.1% phosphoric acid, and 39% water. The flow rate of the mobile phase was 1.2 mL/min.

As summarized in Table 1, the experimental runs were carried out at six temperatures (80, 90, 100, 105, 110, and 120°C), two different initial values of *p*-xylene concentration (4 and 6 mol/kg sol), while maintaining fixed the initial *p*-tolualdehyde concentration (0.11 mol/kg sol). Each run was performed up to conversion values of about 18% in order to prevent the formation of higher oxidation products. The reproducibility of the experimental runs was verified by repeating each of them at least twice. By repeating the experimental run 11 with various stirring speeds (runs 10 and 12), we found that the influence of this variable on the product distribution was negligible and therefore all the other runs were performed at 800rpm. The main products of the oxidations were: *p*-tolualdehyde (TALD), *p*-toluoalcohol (TALC), and *p*-toluic acid (TA).

Lumped Kinetic Scheme and Reactor Modeling

Several detailed mechanisms for *p*-xylene liquid phase catalytic oxidation have been proposed in the literature (cf. Emanuel and Gal, 1986). In general, these are based on the classical free radical chain mechanism involving initiation, propagation, catalytic propagation, and termination steps. However, as discussed in the introduction, the proposed mechanisms are quite complex, and the development of kinetic models, which describe in detail each elementary reaction, appears to be not feasible in practice, due to both experimental and computational difficulties.

Therefore, by taking into account only the reactions leading to the most important intermediate and final products according to the experimental evidence, the following lumped kinetic scheme for *p*-xylene oxidation to *p*-toluic acid is proposed:

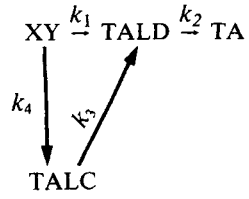

(1)

where XY stands for *p*-xylene, TALD for *p*-tolualdehyde, TA for *p*-toluic acid, TALC for *p*-toluoalcohol, and each reaction involves the addition of 1/2 O_2. Note that in this kinetic scheme the catalyst concentration does not appear explicitly. Its effect on the kinetics of the process has not been investigated in this work, where all the experimental runs have been performed at constant catalyst concentration. In order to account for the effect of this variable, one should suitably change the apparent kinetic constants of the lumped scheme. As discussed in the introduction, the kinetics of each of the lumped reactions above is assumed zeroth-order with respect to oxygen and first-order with respect to the liquid reactant.

In developing the reactor model, it is necessary to describe the transport of oxygen from the gas phase to the liquid phase where reactions (Eq. 1) occur. This is done by using the film model (cf. Carrá and Morbidelli, 1987), which, accounting for the evaporation at the gas-liquid interface and assuming isothermal conditions, can be written in dimensionless form as follows:

$$\xi_i \frac{d^2 \phi_{if}}{d x^2} = -Ha^2 \sum_{j=1}^{NR} \nu_{ij} p_j f_j \tag{2}$$

with boundary conditions (BCs) for the dissolved oxygen:

$$-\frac{d \phi_{O_2 f}}{d x} = \epsilon - \psi \phi^{*}_{O_2 f} \quad \text{at} \quad x = 0 \tag{3}$$

$$\phi_{O_2 f} = \phi_{O_2 \ell} \quad \text{at} \quad x = 1 \tag{4}$$

and for the volatile liquid reactants:

$$-\xi_i \frac{d \phi_{if}}{d x} = \sigma_i - \tau_i \phi^{*}_{if} \quad \text{at} \quad x = 0 \tag{5}$$

$$\phi_{if} = \phi_{i\ell} \quad \text{at} \quad x = 1 \tag{6}$$

where ϕ_{if}, $\phi_{i\ell}$, ϕ^{*}_{if} represent the dimensionless concentration for the ith component in the liquid film, in the liquid bulk and at the gas-liquid interface, respectively. The dimensionless rate of the jth reaction is given by $p_j f_j = k_j \phi_k / k_1$, where $\phi_k = C_k /$

C_ℓ^o is the dimensionless concentration of the liquid reactant in the jth reaction. The dimensionless quantities are defined as follows:

$$\xi_i=\frac{D_i}{D_{O_2}};\quad \phi_{if}=\frac{C_{if}}{C_\ell^o};\quad \phi_{i\ell}=\frac{C_{i\ell}}{C_\ell^o};\quad \phi_{if}^*=\frac{C_{if}^*}{C_\ell^o};\quad x=\frac{s}{\delta}$$

$$Ha^2=\frac{r_1^o D_{O_2}}{k_\ell^2 C_\ell^o};\quad p_j=\frac{r_j^o}{r_1^o};\quad f_j=\frac{r_j}{r_j^o};\quad k_\ell=\frac{D_{O_2}}{\delta}$$

$$\epsilon=\frac{k_{gO_2}\delta}{D_{O_2}C_\ell^o}p_{gO_2};\quad \psi=\frac{k_{gO_2}\delta H_{O_2}}{D_{O_2}}$$

$$p_{gO_2}^*=H_{O_2}C_{O_2f}^*;\quad \phi_{O_2f}^*=\frac{C_{O_2f}^*}{C_\ell^o}$$

$$\sigma_i=\frac{k_{gi}\delta}{D_{O_2}C_\ell^o}p_{gi};\quad \tau_i=\frac{k_{gi}\delta}{D_{O_2}}\frac{p_{si}}{\tilde{p}\ell} \tag{7}$$

where the meaning of all the symbols is reported in the notation. Due to the specific form of the reaction rate f_j, the steady-state film model above can be solved analytically. The obtained solution is rather cumbersome and then only the portion relative to component XY and TA is reported in Table 2.

The dimensionless mass balances for the ith liquid reactant and for oxygen in the bulk liquid phase can be written as follows:

$$\frac{d\,\phi_{i\ell}}{d\,\vartheta}=\xi_i\left[\left(\frac{d\,\phi_{if}}{d\,x}\right)_{x=0}-\left(\frac{d\,\phi_{if}}{d\,x}\right)_{x=1}\right]+\alpha\,Ha^2\sum_{j=1}^{NR}\nu_{ij}\,p_j f_j \tag{8}$$

$$\frac{d\phi_{O_2\ell}}{d\,\vartheta}=-\left(\frac{d\,\phi_{O_2f}}{d\,x}\right)_{x=1}-\alpha\,Ha^2\,\frac{1}{2}\sum_{j=1}^{NR}p_j f_j \tag{9}$$

with initial conditions:

$$\phi_{i\ell}=\phi_{i\ell}^o \quad \text{at} \quad \vartheta=0 \tag{10}$$

where

$$\vartheta=\frac{t\,k_\ell a_v}{\epsilon_\ell-a_v\delta};\quad \alpha=\frac{\epsilon_\ell-a_v\delta}{a_v\delta}. \tag{11}$$

The term $\xi_i(\phi_{if}')_{x=0}$ in Eq. 8 represents the mass flux of liquid reactant leaving the liquid film at the gas-liquid interface $x=0$, which is condensed by the condenser and recycled back to the liquid bulk in the reactor.

All the calculations were carried out by neglecting the partial pressure of the liquid reactants in the gas phase, that is, $\sigma_i=0$ in the BCs (5), and assuming the oxygen partial pressure equal to the inlet value. This assumption was checked *a posteriori*, by verifying, through appropriate gas mass balances, that the oxygen depleted in the gaseous phase was only a small percentage (at most 5%) of the fed oxygen. The steady-state film model Eqs. 2-6 and the overall liquid mass balances (Eqs. 8-11) were solved simultaneously using a standard numerical package (IMSL Math/Library, 1989).

It is worth mentioning that, when dealing with zeroth-order reactions, care must be taken in setting all the reaction rates equal to zero when the oxygen concentration in the liquid film drops to zero. This situation occurs when the reaction is very fast compared to the diffusion rate of the gaseous reactant in

Table 2. Analytical Solution of the Steady-State Film Model (Eqs. 2-6) for the Lumped Kinetic Scheme (1): A = XY, B = TALD, C = TA, and D = TALC

$$\phi_{Af}(x)=\phi_{A\ell}\exp[a_1(1-x)]+\frac{\sinh[a_1(x-1)]}{\cosh(a_1)}\left[\phi_{A\ell}\exp(a_1)-\frac{\sigma_A-\tau_A\phi_{Af}^*}{a_1\xi_A}\right]$$

$$\phi_{Af}^*=\frac{\phi_{A\ell}\exp(a_1)-\left[\phi_{A\ell}\exp(a_1)-\dfrac{\sigma_A}{p_2\xi_A}\right]tgh\ (a_1)}{1+\dfrac{\sigma_A}{p_2\xi_A}\,tgh\ (a_1)};\quad a_1=\sqrt{Ha^2(1+p_4)/\xi_A}$$

$$\phi_{Cf}(x)=\phi_{C\ell}-\frac{\xi_B}{\xi_C}[\phi_{Bf}(x)-\phi_{B\ell}]-\frac{p_2}{\xi_C}\frac{\phi_A\xi_A}{\xi_A p_2-\xi_B(1+p_4)}\left(\frac{\xi_A}{(1+p_4)}-\frac{\xi_B}{p_2}\right)\left[\frac{\phi_{Af}(x)}{\phi_{A\ell}}-1\right]$$

$$+(1-x)\frac{p_2Ha^2}{\xi_C}\left\{\frac{\sigma_C-\tau_C\phi_{Cf}^*}{p^2Ha^2}+\frac{\xi_A\left[1-\dfrac{\xi_B(1+p_4)}{\xi_A p_2}\right]}{\xi_A p_2-\xi_B(1+p_4)}\frac{(\sigma_A-\tau_A\phi_{Af}^*)}{Ha^2(1+p_4)}+\frac{(\sigma_B-\tau_B\phi_{Bf}^*)}{\xi_B}\right\}$$

$$\phi_{Cf}^*=\left\{\phi_{C\ell}-\frac{\xi_B}{\xi_C}[\phi_{Bf}^*-\phi_{B\ell}]-\frac{p_2}{\xi_C}\frac{\phi_A\xi_A}{\xi_A p_2-\xi_B(1+p_4)}\left(\frac{\xi_A}{(1+p_4)}-\frac{\xi_B}{p_2}\right)\left[\frac{\phi_{Af}^*}{\phi_{A\ell}}-1\right]\right.$$

$$\left.+\frac{p_2Ha^2}{\xi_C}\left[\frac{\sigma_C}{p_2Ha^2}+\frac{\xi_A\left[1-\dfrac{\xi_B(1+p_4)}{\xi_A p_2}\right]}{\xi_A p_2-\xi_B(1+p_4)}\frac{(\sigma_A-\tau_A\phi_{Af}^*)}{Ha^2(1+p_4)}+\frac{(\sigma_B-\tau_B\phi_{Bf}^*)}{\xi_B}\right]\right\Big/\left(1+\frac{\tau_C}{\xi_C}\right)$$

the liquid film. In this case, the reaction goes to completion within the liquid film, while for slower reaction rates, it takes place both in the liquid film and in the liquid bulk. When the reaction rate is much slower than the rate of diffusion, most of the reaction occurs in the liquid bulk and the contribution of the reaction in the liquid film may be neglected. These three regimes have been identified and separately described by Hashimoto et al. (1968) for the case of two consecutive reactions both taken as first-order with respect to the liquid reactant and zeroth-order with respect to the dissolved gaseous species and more recently by Landau (1990) for a single gas absorption accompanied by zeroth-order chemical reaction.

In order to describe in a continuous fashion the transition between these regimes, which may occur during a single reaction batch due to the depletion of the liquid reactants, a unified approach to the evaluation of oxygen mass transfer has to be introduced (Servida et al., 1994). This is based on the comparison between the oxygen flux entering the liquid bulk and the maximum possible rate of oxygen consumption in the liquid bulk. Three situations may arise.

Case 1. The oxygen flux is larger than the maximum possible rate of oxygen consumption in the liquid bulk, that is:

$$-2\left(\frac{d\,\phi_{O_2 f}}{dx}\right)_{x=1} > \alpha\, Ha^2 \sum_{j=1}^{NR} p_j f_j \tag{12}$$

In this case the reactor is in the chemically controlled regime. Most of the oxidation process occur in the liquid bulk, since the oxygen entering the liquid bulk is sufficient to sustain the reaction. The oxygen concentration in the liquid bulk is larger than zero, and the liquid mass balances (Eqs. 8–9) retain their original form.

Case 2. The oxygen flux is smaller than the maximum possible rate of oxygen consumption in the liquid bulk, that is:

$$-2\left(\frac{d\phi_{O_2 f}}{dx}\right)_{x=1} < \alpha\, Ha^2 \sum_{j=1}^{NR} p_j f_j \tag{13}$$

In this case the oxidation process occurs both in the liquid film and in the liquid bulk. All the oxygen entering the liquid bulk is depleted by the oxidation reactions and its concentration is then equal zero. The amount of oxygen consumed by each reaction is computed according to its relative rate with respect to that of all the others. Thus, the liquid mass balances (Eqs. 8–9) take the following form:

$$\frac{d\,\phi_{if}}{d\vartheta} = \xi_i \left[\left(\frac{d\,\phi_{if}}{dx}\right)_{x=0} - \left(\frac{d\,\phi_{if}}{dx}\right)_{x=1}\right] - 2\left(\frac{d\,\phi_{O_2 f}}{dx}\right)_{x=1} \sum_{j=1}^{NR} \nu_{ij} \frac{p_j f_j}{\sum_{k=1}^{NR} p_k f_k} \tag{14}$$

$$\frac{d\,\phi_{O_2 \ell}}{d\,\vartheta} = 0 \tag{15}$$

Case 3. Oxygen is completely depleted within the liquid film, so that:

$$\phi_{O_2 \ell} = \left(\frac{d\phi_{O_2 f}}{dx}\right)_{x=1} = \sum_{j=1}^{NR} p_j f_j = 0 \tag{16}$$

In this case no reaction occurs in the liquid bulk, and also the film (Eqs. 2–6) needs to be modified by considering that only in a portion of the liquid film (that is, the reactive liquid film) the reaction is taking place. This situation is discussed in detail by Servida et al. (1994) but it is not pursued here any further since it never arose in the experimental runs considered in this work.

It is worth noting that the model equations above contain a large number of physicochemical parameters which need to be evaluated in order to compare the model results with the experimental data. Most of the parameters, with the exception of the rate constants of the four lumped reactions (Eq. 1) and the liquid phase mass-transfer coefficient k_ℓ, have been evaluated from independent literature relationships. The obtained values of the physicochemical parameters, together with the values of the operating conditions and of the dimensionless model parameters, are summarized in Table 3 for the experimental run 11. The reaction rate constants and the liquid film mass-transfer coefficient have been evaluated by comparison with the experimental data as described in the next section.

Comparison with Experimental Data

In order to better understand the behavior of the reactor, it is convenient to first consider the overall oxygen uptake, U_{O_2} computed through the following relationship:

$$U_{O_2} = \frac{1}{2}\left[C_{TALD} - C^{o}_{TALD} + 2C_{TA} + C_{TALC}\right] \tag{17}$$

where C_{TALD}, C_{TA} and C_{TALC} represent the experimentally measured concentrations of the reaction products. A typical plot of the overall amount of oxygen consumed in the liquid phase as a function of time is shown in Figure 2 for different temperature values. From the slope of these curves it is possible to obtain at each time value, the overall rate of oxygen uptake, R_{O_2}. In particular, the initial uptake values, $R^0_{O_2}$, obtained at time $t = 0$, are shown in Figure 3 as a function of temperature. Note that two sets of experimental data are reported, depending upon whether pure oxygen or air was fed to the reactor, but all involving the same initial composition of the liquid phase.

From the Arrhenius-like plot of $R^0_{O_2}$ as a function of temperature shown in Figure 3, some interesting conclusion about the reactor operating regimes can be drawn. At low temperature values, the reactor operates in the chemically controlled regime. The rate of oxygen uptake is the same whether pure oxygen or air is used, thus confirming that the chemical reaction is zeroth-order with respect to oxygen. Moreover, the apparent activation energy is equal to about 15 kcal/mol, that is, a value typical of oxidation reactions. Note that this value is in good agreement with those reported in the literature for *p*-xylene oxidation in the presence of water (cf. Hronec and Ilavsky, 1982; Hronec et al., 1985; Hronec and Hrabe, 1986). On the other hand, at higher temperature values diffusional limitations become important. These arise first in the experiments performed with air, as indicated by the deviation from linearity exhibited by the corresponding data in the Arrhenius

Table 3. Model Parameter Values for Experimental Run 11

Parameter	Value	Reference
a_v	2.5 cm^{-1}	Sridhar and Potter (1980)
C_l^0	3.9 $\times 10^{-3}$ $mol \cdot cm^{-3}$	
D_i	3.4 $\times 10^{-5}$ $cm^2 \cdot s^{-1}$	Wilke and Chang (1955)
D_{O_2}	9.85 $\times 10^{-5}$ $cm^2 \cdot s^{-1}$	Wilke and Chang (1955)
H_{O_2}	4.4 $\times 10^5$ $cm^3 \cdot atm \cdot mol^{-1}$	
Ha	7.7 $\times 10^{-3}$	
k_{gXY}	9.9 $\times 10^{-5}$ $mol \cdot s^{-1} \cdot atm^{-1} \cdot cm^{-2}$	Newman (1931)
k_{gTALD}	9.3 $\times 10^{-5}$ $mol \cdot s^{-1} \cdot atm^{-1} \cdot cm^{-2}$	Newman (1931)
k_{gTA}	8.7 $\times 10^{-5}$ $mol \cdot s^{-1} \cdot atm^{-1} \cdot cm^{-2}$	Newman (1931)
k_{gTALC}	9.2 $\times 10^{-5}$ $mol \cdot s^{-1} \cdot atm^{-1} \cdot cm^{-2}$	Newman (1931)
k_{gO_2}	0.048 $mol \cdot s^{-1} \cdot atm^{-1} \cdot cm^{-2}$	Newman (1931)
p_{gi}	0 atm	
p_{sXY}	0.44 atm	Reid et al. (1977)
p_{sTALD}	0.074 atm	Reid et al. (1977)
p_{sTA}	0 atm	Reid et al. (1977)
p_{sTALC}	0.04 atm	Reid et al. (1977)
p_{gO_2}	1 atm	
δ	2.11 $\times 10^{-3}$ cm	
ϵ_l	0.9	Carrá and Morbidelli (1987)
ρ_l	0.98 $\times 10^{-3}$ $kg_{sol} \cdot cm^{-3}$	
$\tilde{\rho}_l$	7.96 $\times 10^{-3}$ $mol \cdot cm^{-3}$	

plot in Figure 3. A further support is given by the apparent activation energy value, which can be estimated from the two data at higher temperature for air oxidation as given by about 4 kcal/mol, a value typical of mass-transfer limited processes. The experimental data relative to pure oxygen seem to lie on the same straight line on the Arrhenius plot in Figure 3, thus indicating that in this case the reactor operates in the chemically controlled regime in the entire temperature range. This behavior can be explained by considering that the maximum possible rate of mass transfer in the runs with oxygen is about five times larger than that for the runs with air. Accordingly, since diffusional limitations for the runs with air occur when $R^0_{O_2} \simeq 0.0025$ mol/kg_{sol} min, we could expect the same limitations to occur when the rate of oxygen consumption is roughly five times larger. This could be obtained either at higher temperature values (presumably at $T \simeq 130°C$) or at larger catalyst concentration values. Neither of these conditions has been investigated experimentally in this work.

As mentioned earlier, our aim is to represent all the obtained experimental data with a single model which covers all possible regimes of the reactor. In order to obtain a reliable estimate of the involved physicochemical parameters, it is convenient to adopt the following procedure, which is suggested by the observations about the reactor regime reported above. First, we evaluate the rate constants of the four lumped reactions (Eq. 1) by considering only the experimental data using oxygen in the feedstream, where diffusional resistances are not involved. For this we use the model above with $Ha = 0$, which

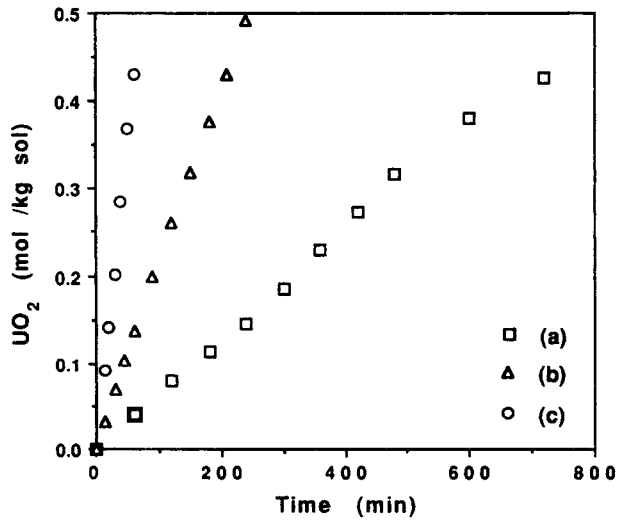

Figure 2. Overall oxygen uptake, UO_2, as a function of time for different temperature values: runs 1, 5, and 14 in Table 1.

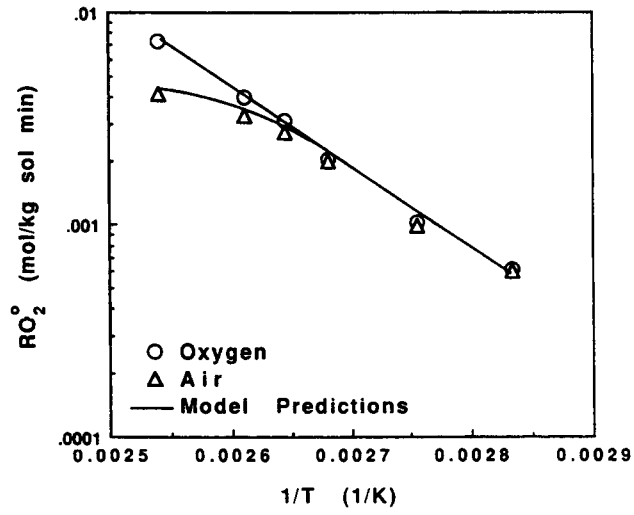

Figure 3. Comparison between calculated and experimental values of the initial uptake rate of oxygen, RO_2^0, as a function of temperature and oxygen partial pressure: runs 1 to 6, 8, 9, 11, and 13 to 15 in Table 1.

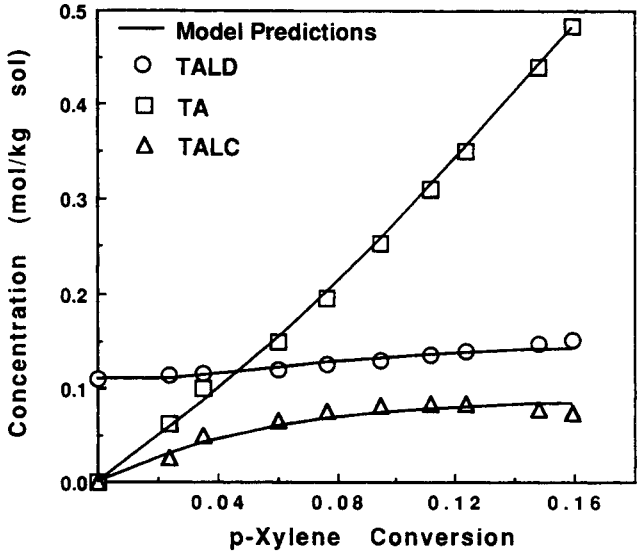

Figure 4. Comparison between calculated and experimental values of the product concentrations as a function of *p*-xylene conversion: run 11 in Table 1.

then reduces to a homogeneous model. Moreover, we first consider the evolution of the product composition using *p*-xylene conversion rather than time as the independent variable, as shown in Figure 4. It is readily seen that these data depend on the ratios of the rate constants rather than on the absolute rate constants themselves. Thus, using a nonlinear least-square procedure, the values of the reactivity ratios $p_2 = k_2/k_1$, $p_3 = k_3/k_1$ and $p_4 = k_4/k_1$ are estimated at each temperature value. A typical comparison between model results and experimental data is shown in Figure 4, while the estimated values of the reactivity ratios are summarized as a function of temperature in Table 4, together with the corresponding value of the average percentage error, η_1 arising from the fitting procedure. Note that all the experimental runs considered refer to the same values of initial concentration of *p*-xylene and *p*-tolualdehyde, that is, 4 and 0.11 mol/kg sol, respectively.

Next, the value of the rate constant k_1 has been estimated by fitting the evolution of the product composition as a function of time, and using the reactivity values in Table 4. The obtained values of k_1 at each temperature value are reported in Table 4, together with the corresponding average percentage error, η_2. The comparison between model results and measured data is shown in Figures 5a–f, where it can be seen that the obtained agreement is in general satisfactory. It is worth mentioning that, even though not shown here, also the experimental runs with air in the feed streams, which fall in the chemically controlled regime (that is, runs 2, 4, 6, and 9 in Table 1) are equally well reproduced by the model. This allows us to conclude that the lumped kinetic scheme (Eq. 1) retains a level of process description detailed enough to characterize the distribution of the most important final products. Moreover, from the Arrhenius plot shown in Figure 6a, it can be seen that the absolute values of the rate constant k_1 in Table 4 lie on a straight line whose slope provides an apparent activation energy value of 14.6 kcal/mol, which is in good agreement with those reported in the literature (cf. Bang and Chandalia, 1974 for methyl-*p*-toluate oxidation; Chen et al., 1985 for *o*-xylene oxidation). Similar plots are obtained for the reactivity ratios p_2, p_3, and p_4 as shown in Figure 6b.

We can now turn to the evaluation of the liquid-phase mass-transfer coefficient, k_ℓ. In particular, we consider the experimental run at 110°C with air in the feedstream (that is, run 13 in Table 1) where, as it is clearly seen in Figure 3, the shift from the kinetic to the diffusion controlled regime is occurring. Since the reaction rate constants have already been estimated, the experimental data measured in these conditions are best suited to estimate the coefficient, k_ℓ. In particular, we use the complete heterogeneous model and estimate the parameter k_ℓ (that is, Ha) by fitting the measured values of the oxygen amount absorbed in the liquid phase as a function of time, obtained by operating the reactor both with pure oxygen and air at 110°C as shown in Figure 7. It should be noted that the sought value of k_ℓ is a rather specific one since it makes the heterogeneous model predict the shift from the kinetic (oxygen run) to the mass-transfer regime (air run) by only changing the oxygen partial pressure in the BC (Eq. 3), while maintaining fixed the kinetic parameters, k_1, k_2, k_3, and k_4 estimated above. A comparison between experimental data and model predictions at 110°C, for the best fitting value of the liquid mass-transfer coefficient (k_ℓ = 2.8 cm/min) is shown in Figure 7. This compares reasonably well with the values given by semi-empirical literature relationships, such as k_ℓ = 4.86 cm/min obtained through the correlation of Calderbank and Moo-Young (1961).

The value of k_ℓ at temperature values other than 110°C, can be estimated from the k_ℓ value obtained above using the following relationship:

$$k_\ell^T = k_\ell^{110^\circ} \left(\frac{D_{O_2}^T}{D_{O_2}^{110^\circ}} \right) \tag{18}$$

which can be deduced from the correlations available in the literature for drops or bubbles in stirred solutions (cf. Calderbank and Moo-Young, 1961). We can now compute the initial rate of oxygen uptake, $R_{O_2}^0$ as a function of temperature, by considering the reactor fed both with pure oxygen and air.

Table 4. Estimated Values of the Kinetic Parameters of Lumped Kinetic Scheme (Eq. 1)

T (°C)	$k_1 \times 10^4$ (min^{-1})	η_2 (%)	$p_2 = k_2/k_1$	$p_3 = k_3/k_1$	$p_4 = k_4/k_1$	η_1 (%)
80	1.37	2.9	35.6	13.5	0.37	2.1
90	2.33	6.3	32.8	15.1	0.41	6.6
100	4.04	3.8	35.3	22.6	0.61	2.5
105	6.54	3.3	32.7	19.9	0.50	3.5
110	7.94	4.9	37.1	25.6	0.70	4.9
120	12.5	7.4	41.1	23.7	0.76	7.4

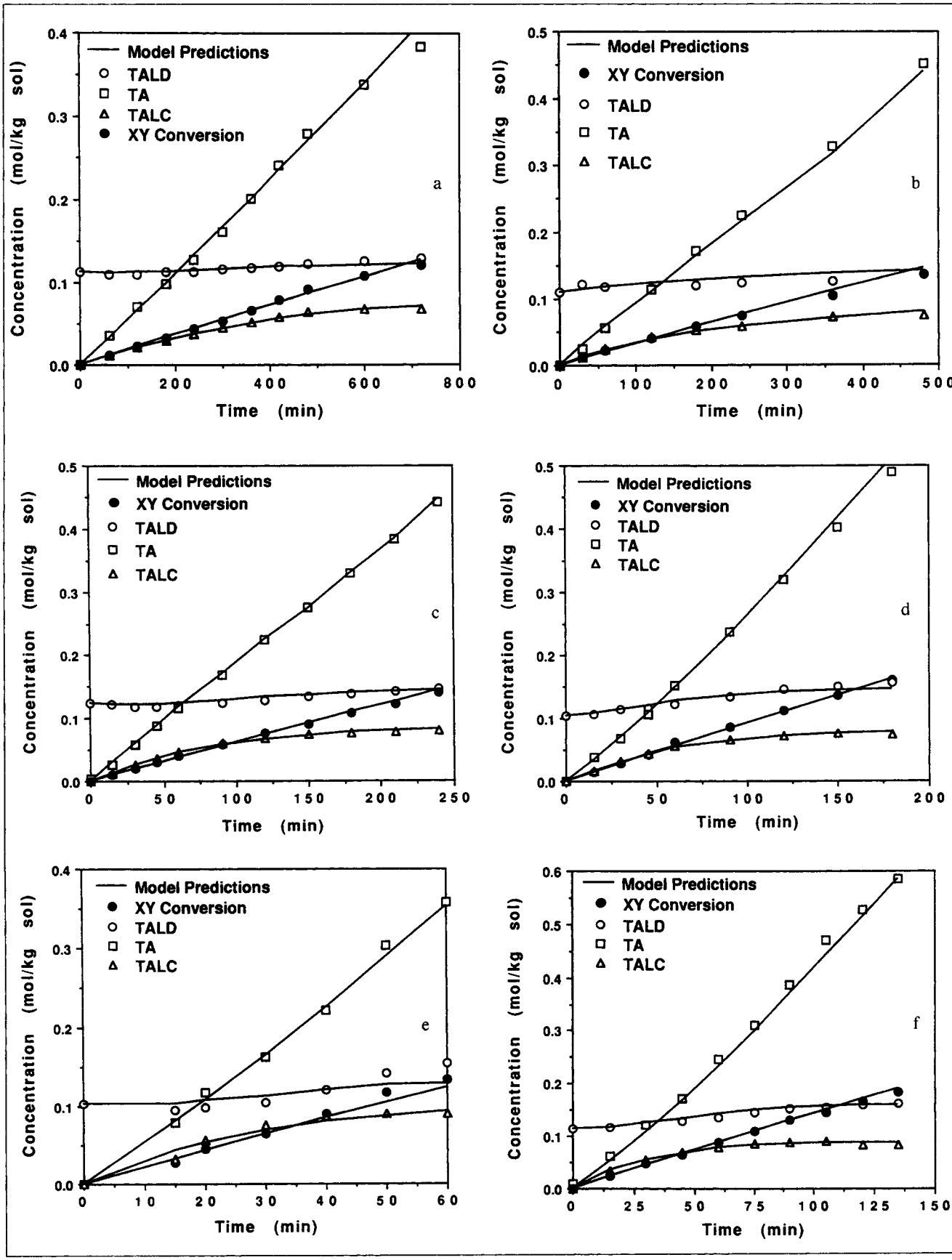

Figure 5. Calculated vs. experimental values of product concentrations as a function of time for various temperatures: runs 1 (a), 3 (b), 5 (c), 8 (d), 11 (e), and 14 (f) in Table 1.

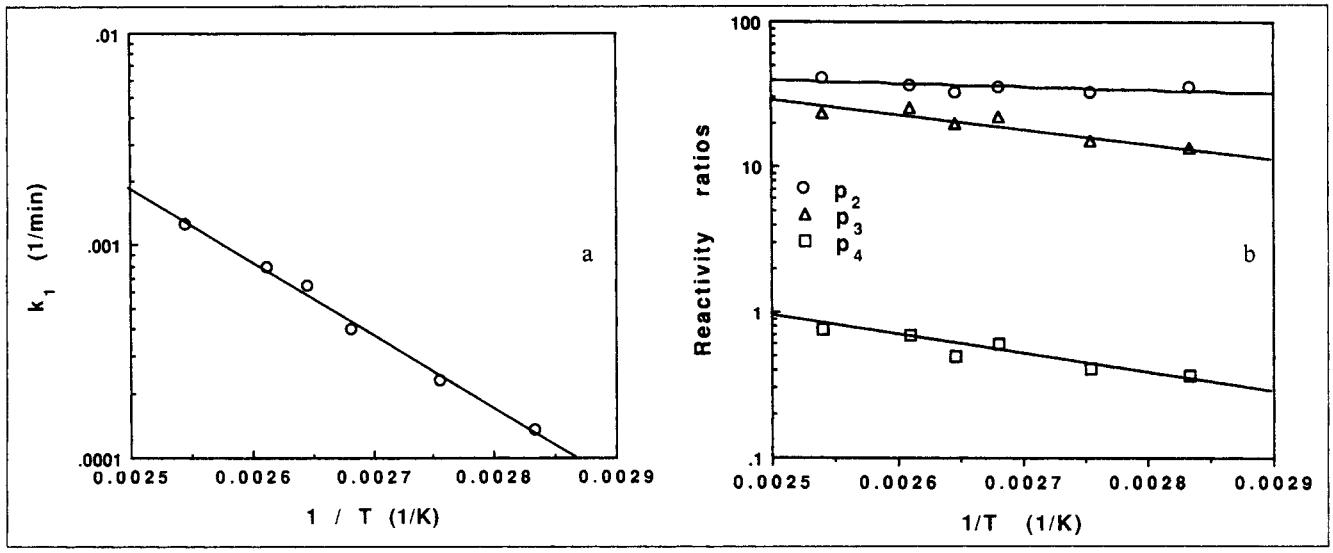

Figure 6. Arrhenius plots for reaction rate constant k_1 of lumped kinetic scheme (Eq. 1) and for reactivity ratios p_2, p_3, and p_4.

The obtained values are compared with the corresponding experimental data in Figure 3. Note that the transition from oxygen to air (that is, the effect of diffusion limitation) at 110°C leads to a decrease of initial oxygen uptake $R^0_{O_2}$ equal to about 20%. This corresponds to the data shown in Figure 7, which have been fitted with the model in order to estimate k_l. On the other hand, at T = 120°C the change in the value of $R^0_{O_2}$ is much larger, that is, about 40%, and it is well predicted by the model. A detailed comparison of the measured and calculated product composition as a function of time is shown in Figure 8 for these two runs (that is, runs 13 and 15 in Table 1). Moreover, for decreasing the temperature values, the reactor enters the chemically controlled region and the model predictions become independent of the oxygen partial pressure. This is in agreement with the experimental data in Figure 3,

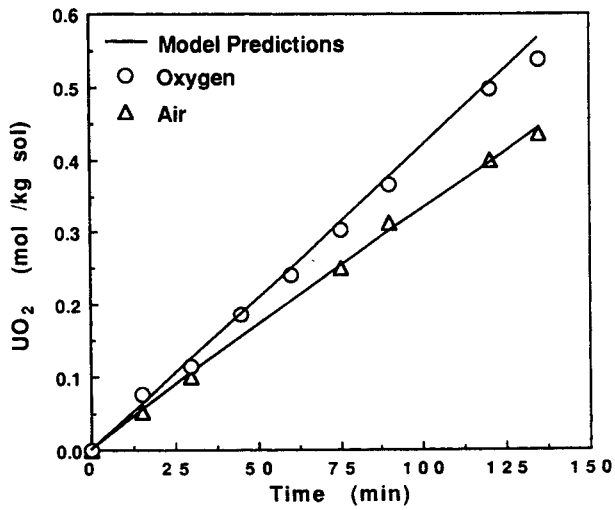

Figure 7. Calculated vs. experimental values of overall oxygen uptake, UO_2, as a function of time for oxygen partial pressures: run 11 (O) and run 13 (Δ) in Table 1.

where it can be seen that the initial oxygen uptake values, $R^0_{O_2}$ measured when feeding the reactor with pure oxygen or with air are coincident. It is worth mentioning that the computed values of the Hatta number, range from 3.98×10^{-4} at 80°C to 9.14×10^{-4} at 120°C. These are rather small values, in agreement with the common understanding which classifies *p*-xylene oxidation as a typical slow reaction.

In order to test the assumption of first-order kinetics with respect to the liquid reactant for all the reactions in the lumped kinetic scheme (Eq. 1), an experimental run in the chemically controlled regime with different initial *p*-xylene concentration has been considered. In particular, we consider pure oxygen feed, T = 100°C and the initial concentration of *p*-xylene equal to 6 mol/kg sol, while that of *p*-tolualdehyde remains unchanged, that is, 0.11 mol/kg sol (run 7 in Table 1). Note that no parameter has been changed in the model, whose results should then be regarded as predictions of the actual reactor behavior. The comparison with the data measured experimentally is shown in Figure 9, where it is seen that the agreement is satisfactory (average percentage error $\eta = 8.9\%$).

Conclusion

A model for the simulation of semibatch gas liquid reactors for *p*-xylene catalytic oxidation to *p*-toluic acid has been developed. It is based on the lumping of the complex radical chain mechanism of the oxidation process into an appropriate kinetic scheme, whose reactions are assumed to be zeroth-order with respect to oxygen and first-order with respect to the liquid reactant. The model accounts properly for the zeroth-order kinetics by checking at each time if the oxygen flux entering the liquid bulk is sufficient to sustain the reaction, that is, it is larger or not than the maximum possible rate of consumption in the liquid bulk. This allows us to describe in a continuous fashion the transition which may take place in the reactor regime, depending upon the operating conditions and the depletion of the liquid reactants. With respect to previous studies on gas-liquid oxidation reactors (cf. Jacobi and Baerns, 1983),

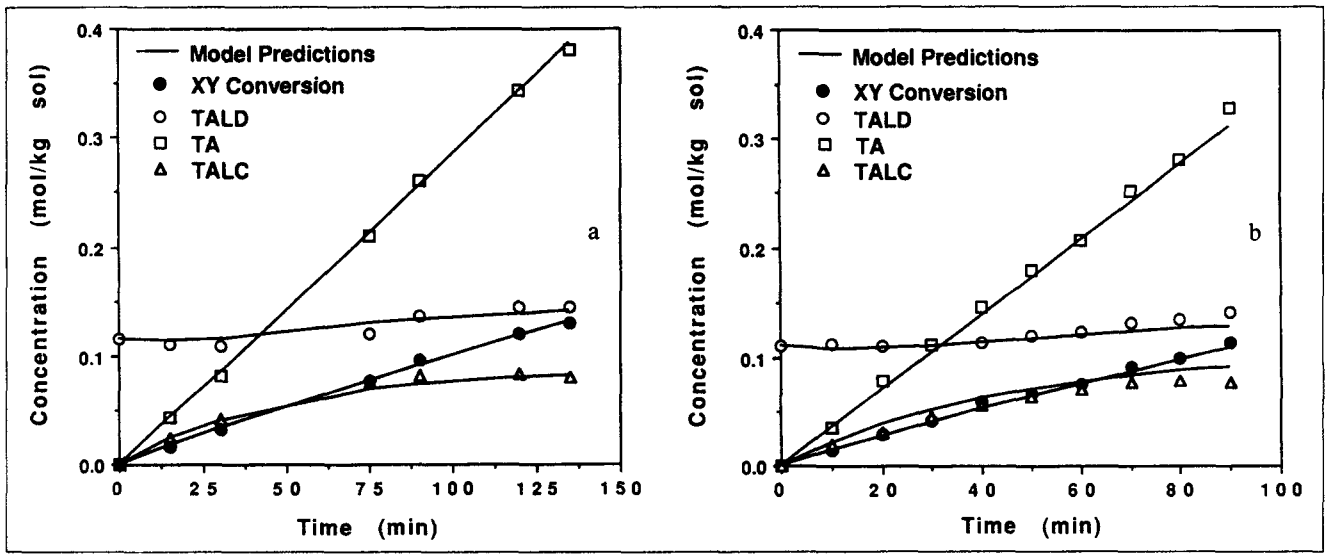

Figure 8. Calculated vs. experimental values of product concentrations as a function of time: runs 13 (a) and 15 (b) in Table 1.

the model developed in this work does not require to specify *a priori* the reactor operating regime, since it properly accounts for the interaction between chemical reactions and transport processes for all possible operating conditions. This allowed to verify that, at least for the oxidation process here considered, the experimental data are consistent with the zeroth-order kinetics in the liquid phase, when diffusional limitations are properly accounted for.

Acknowledgments

The financial support of the Italian Consiglio Nazionale delle Ricerche, Progetto Finalizzato Chimica Fine and of the Regione Autonoma della Sardegna is gratefully acknowledged. The assistance of Mr. A. Viola in setting up the analytical method is also acknowledged.

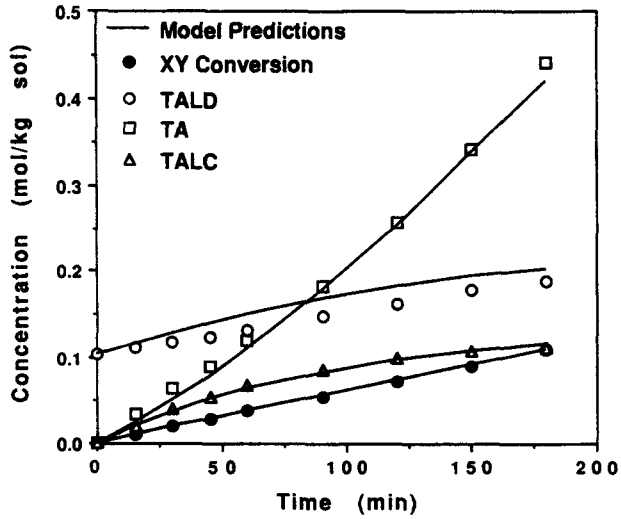

Figure 9. Comparison between predicted and experimental values of product concentrations as a function of time: run 7 in Table 1.

Notation

a_v = gas-liquid interfacial area per unit volume, cm^{-1}
C_i = concentration of the ith component, mol/cm^3
C_ℓ^o = reference concentration for the liquid phase, mol/cm^3
D_i = diffusion coefficient of the ith liquid component, cm^2/s
f_j = r_j/r_j^0
H_{O_2} = Henry's constant for oxygen, cm^3 atm/mol
Ha = Hatta number, $(r_1^0 D_{O_2}/k_\ell^2 C_\ell^o)^{0.5}$
k_j = rate constant for the jth reaction, min^{-1}
k_ℓ = oxygen liquid side mass-transfer coefficient, cm/min
k_{gi} = gas side mass-transfer coefficient for the ith component, $mol \cdot s^{-1} \cdot atm^{-1} \cdot cm^{-2}$
N = rotating speed, rpm
NR = reaction number
p_j = $r_j^0/r_1^0 = k_j/k_1$
p_{gi} = partial pressure of the ith component, atm
p_{si} = vapor pressure of the ith component, atm
r_j = rate of the jth reaction, $mol/cm^3 s$
R_{O_2} = overall oxidation rate, mol/kg sol min
$R_{O_2}^0$ = overall oxidation rate at $t=0$, mol/kg sol min
s = distance from the gas-liquid interface, cm
t = time, s
T = temperature, K
U_{O_2} = overall oxygen uptake, mol/kg sol
x = s/δ

Greek letters

α = ratio between the liquid bulk volume and the liquid film volume, $(\epsilon_\ell - a_v\delta)/a_v\delta$
δ = liquid film thickness, D_{O_2}/k_ℓ, cm
ϵ = $k_{gO_2}\delta p_{gO_2}/D_{O_2} C_\ell^o$
ϵ_ℓ = liquid holdup
η = average percentage error
ϑ = dimensionless time, $t\, k_\ell a_v/(\epsilon_\ell - a_v\, \delta)$
ν_{ij} = stoichiometric coefficient of the ith component in the jth reaction
ξ_i = D_i/D_{O_2}
ρ_ℓ = density of the liquid mixture, kg_{sol}/cm^3
$\tilde{\rho}_\ell$ = molar density of the liquid mixture, mol/cm^3
σ_i = $k_{gi}\, \delta\, p_{gi}/D_{O_2} C_\ell^o$

τ_i = $k_{gi}\,\delta\,p_{si}/D_{O_2}\,\tilde{\rho}_\ell$
ϕ_i = dimensionless concentration of the ith component, C_i/C_i^o
ψ = $k_{gO_2}\,\delta\,H_{O_2}/D_{O_2}$

Subscripts

f = liquid film
g = gaseous phase
i = component index
j = reaction index
ℓ = liquid phase
O_2 = oxygen

Superscripts

o = reference or initial conditions
$*$ = gas-liquid interface

Literature Cited

Astarita, G., D. W. Savage, and A. L. Bisio, *Gas Treating with Chemical Solvents*, John Wiley, New York (1983).

Bang, S. R., and S. B. Chandalia, "Liquid Phase Oxidation of Methyl-*p*-Toluate to Monomethyl Terephtalate," *Ind. Chem. Eng.*, **16**, T92 (1974).

Calderbank, P. H., and M. B. Moo-Young, "The Continuous Phase Heat and Mass Transfer Properties of Dispersions," *Chem. Eng. Sci.*, **16**, 39 (1961).

Cavalieri d'Oro, P., E. Danoczy, and P. Roffia, "On the Low Temperature Oxidation of *p*-Xylene," *Oxidation Communications*, **1**, 153 (1980).

Carrá, S., and M. Morbidelli, "Gas-Liquid Reactors," in *Chemical Reaction and Reactor Engineering*, J. J. Carberry and A. Varma, eds., Marcel Dekker, New York and Basel, pp. 545-666 (1987).

Chen, Z., G. Li, W. Li, L. Dai, Y. Niu, J. Hu, J. Gu, X. Mao, and M. Li, "The Kinetics of the Oxidation of *o*-Xylene," *Int. Chem. Eng.*, **25**, 738 (1985).

Doraiswamy, L. K., and M. M. Sharma, *Heterogeneous Reactions: Analysis, Examples and Reactor Design, Vol. II*, John Wiley, New York (1984).

Emanuel, N. M., and D. Gal, *Modelling of Oxidation Processes*, Akademiai Kiado, Budapest (1986).

Hashimoto, K., M. Teramoto, T. Nagayasu, and S. Nagata, "The Effects of Mass Transfer on the Selectivity of Gas-Liquid Reactions," *J. Chem. Eng. Jap.*, **2**, 132 (1968).

Hobbs, C. C., E. H. Drew, H. A. Van't Hof, F. G. Mesich, and M. J. Onore, "Mass-Transfer Rate-Limitation Effects in Liquid-Phase Oxidation," *Ind. Eng. Chem. Prod. Res. Dev.*, **11**, 220 (1972).

Hronec, M., and J. Ilavsky, "Oxidation of Polyalkylaromatic Hydrocarbons. 12. Technological Aspect of *p*-Xylene Oxidation to Terephtalic Acid in Water," *Ind. Eng. Prod. Chem. Res. Dev.*, **21**, 455 (1982).

Hronec, M., Z. Cvengrosova, and J. Ilavsky, "Kinetics and Mechanism of Cobalt-Catalyzed Oxidation of *p*-Xylene in the Presence of Water," *Ind. Eng. Process Des. Dev.*, **24**, 787 (1985).

Hronec, M., and Z. Hrabe, "Liquid-Phase Oxidation of *p*-Xylene Catalyzed by Metal Oxides," *Ind. Eng. Prod. Chem. Res. Dev.*, **25**, 257 (1986).

Jacobi, R., and M. Baerns, "The Effect of Oxygen Transfer Limitation at the Gas-Liquid Interface," *Erdoel Kohle Erdgas Petrochem.*, **36**(7), 322 (1983).

Krzysztoforski, A., Z. Woichik, R. Poharecki, and J. Baldyga, "Industrial Contribution to the Reaction Engineering of Cyclohexane Oxidation," *Ind. Eng. Chem. Process Des. Dev.*, **25**, 894 (1986).

Landau, J., "Absorption Accompanied by a Zero-Order Reaction," *Can. J. Chem. Eng.*, **68**, 599 (1990).

Mill, T., and D. G. Hendry, "Kinetics and Mechanisms of Free Radical Oxidation of Alkenes and Olefins in the Liquid Phase," in *Comprehensive Chemical Kinetics, Vol. 1*, C. H. Bamford and C. F. H. Tipper, eds., Elsevier, Amsterdam, pp. 1-87 (1980).

Morbidelli, M., A. Servida, and S. Carrá, "Bimolecular Reactions of General Order in Gas-Liquid Reactors with Volatile Reactants: Applications to the Case of Auto-Oxidation Units," in *Frontiers in Chemical Engineering, Vol. 1*, L. K. Doraiswamy and R. A. Mashelkar, eds., John Wiley Eastern, New Delhi, pp. 440-463 (1984).

Morbidelli, M., R. Paludetto, and S. Carrá, "Gas-Liquid Autoxidation Reactors," *Chem. Eng. Sci.*, **41**, 2299 (1986).

Newman, A. B., "The Drying of Porous Solids: Diffusion Calculations," *AIChE Trans.*, **27**, 310 (1931).

Raghavendrachar, P., and S. Ramachandran, "Liquid-Phase Oxidation of *p*-Xylene," *Ind. Eng. Chem. Res.*, **31**, 453 (1992).

Reid, R. R., J. M. Prausnitz, and T. K. Sherwood, *The Properties of Gases and Liquids*, McGraw-Hill, New York (1977).

Sridhar, T., and O. E. Potter, "Gas Holdup and Bubble Diameters in Pressurized Gas-Liquid Stirred Vessels," *Ind. Eng. Chem. Fundam.*, **19**, 21 (1980).

Servida, A., G. Cao, E. Rombi, and M. Morbidelli, "Engineering Aspects of Gas-Liquid Catalytic Oxidations," Manuscript in preparation (1994).

Sheldon, R. A., and J. K. Kochi, *Metal Catalyzed Oxidation of Organic Compounds*, Academic Press, New York (1981).

Uri, N., *Autoxidation and Antioxidants, Vol. 1*, W. O. Lundberg, ed., Wiley, New York (1961).

Wilke, C. R., and P. Chang, "Correlation of Diffusion Coefficients in Dilute Solutions," *AIChE J.*, **1**, 264 (1955).

Manuscript received Apr. 27, 1993, and revision received Aug. 9, 1993.